

# Chamber properties from transmitral flow: prediction of average and passive left ventricular diastolic stiffness

JENNIFER B. LISAUSKAS, JASVINDAR SINGH,  
ANDREW W. BOWMAN, AND SÁNDOR J. KOVÁCS  
Cardiovascular Biophysics Laboratory, Washington University  
School of Medicine, St. Louis, Missouri 63110

Received 29 December 2000; accepted in final form 5 March 2001

**Lisauskas, Jennifer B., Jasvinder Singh, Andrew W. Bowman, and Sándor J. Kovács.** Chamber properties from transmitral flow: prediction of average and passive left ventricular diastolic stiffness. *J Appl Physiol* 91: 154–162, 2001.—A chamber stiffness ( $K_{LV}$ )-transmitral flow (E-wave) deceleration time relation has been invasively validated in dogs with the use of average stiffness  $[(\Delta P/\Delta V)_{avg}]$ .  $K_{LV}$  is equivalent to  $k_E$ , the (E-wave) stiffness of the parameterized diastolic filling model. Prediction and validation of 1)  $(\Delta P/\Delta V)_{avg}$  in terms of  $k_E$ , 2) early rapid-filling stiffness  $[(\Delta P/\Delta V)_E]$  in terms of  $k_E$ , and 3) passive (postdiastasis) chamber stiffness  $[(\Delta P/\Delta V)_{PD}]$  from A waves in terms of the stiffness parameter for the Doppler A wave ( $k_A$ ) have not been achieved. Simultaneous micromanometric left ventricular (LV) pressure (LVP) and transmitral flow from 131 subjects were analyzed.  $(\Delta P)_{avg}$  and  $(\Delta V)_{avg}$  utilized the minimum LVP-LV end-diastolic pressure interval.  $(\Delta P/\Delta V)_E$  utilized  $\Delta P$  and  $\Delta V$  from minimum LVP to E-wave termination.  $(\Delta P/\Delta V)_{PD}$  utilized atrial systolic  $\Delta P$  and  $\Delta V$ . E- and A-wave analysis generated  $k_E$  and  $k_A$ . For all subjects, noninvasive-invasive relations yielded the following equations:  $k_E = 1,401 \cdot (\Delta P/\Delta V)_{avg} + 59.2$  ( $r = 0.84$ ) and  $k_E = 229.0 \cdot (\Delta P/\Delta V)_E + 112$  ( $r = 0.80$ ). For subjects with diastasis ( $n = 113$ ),  $k_A = 1,640 \cdot (\Delta P/\Delta V)_{PD} - 8.40$  ( $r = 0.89$ ). As predicted,  $k_A$  showed excellent correlation with  $(\Delta P/\Delta V)_{PD}$ ;  $k_E$  correlated highly with  $(\Delta P/\Delta V)_{avg}$ . In vivo validation of average, early, and passive chamber stiffness facilitates quantitative, non-invasive diastolic function assessment from transmitral flow.

diastole; echocardiography; hemodynamics; ventricles; mathematical modeling

IN ACCORDANCE WITH THE LAWS of fluid mechanics, left ventricular (LV) diastolic transmitral flow is generated by the atrioventricular pressure gradient (21, 30). In response to the rapid ( $\sim 100$  ms) development of the maximal pressure gradient, normal mitral valve (MV) leaflets separate widely as early rapid filling of the ventricle ensues, and the Doppler E wave is generated. Diastolic filling occurs in three phases. The first phase is early rapid filling, a phase initiated by a period of mechanical suction ( $dP/dV < 0$ , where P is pressure and V is volume) in all hearts (11), generated by the transient dominance of intracellular [titin (10)] and

extracellular compartment [connective tissue matrix (4, 26)]-driven mechanical recoil over progressive myocardial relaxation. The magnitude of transmitral flow velocity can be modulated by numerous extracardiac factors, such as preload and afterload. The second phase is diastasis; if heart rate is typically  $< 75$  beats/min, this quiescent phase is characterized by an overall balance of forces (e.g., chamber wall, pericardial, thoracic, and similar) manifesting as absence of the atrioventricular pressure gradient and no change in volume. We emphasize that balance of forces during diastasis does not imply absence of forces (24). The third phase, atrial contraction, ensues when contraction of atrial myocardium pulls the MV annulus and aortic root toward the mediastinum, generating a positive atrioventricular pressure gradient, forcing blood into the ventricle ( $dP/dV > 0$ ) and retrogradely into the pulmonary veins. Atrial contraction causes a simultaneous increase in LV pressure (LVP) and volume, and the relative duration of antegrade (transmitral) vs. retrograde (pulmonary vein) flow is related to atrioventricular compliance and pressure (1).

By definition, the slope ( $dP/dV$ ) of the LVP-volume curve is the LV chamber stiffness (19). The diastolic pressure-volume relation is curvilinear (concave upward) in shape, and its slope (i.e., chamber stiffness) increases as the LV end-diastolic pressure (LVEDP) and volume increase. Classically, measurement of this chamber property has required catheterization-based measurement of LVP and the simultaneous change in volume.

Doppler-derived indexes of diastolic function have utilized the pattern of LV filling as seen on transmitral Doppler echocardiographic images (16). Selected indexes derived from this method include peak velocities of early rapid filling (Doppler E wave), atrial contraction (Doppler A wave), and the E-to-A ratio, as well as the acceleration time ( $t_{acc}$ ) and deceleration time ( $t_{dec}$ ).

Diastolic dysfunction has been associated with three types of E-wave patterns: delayed relaxation, pseudo-normalized, and restrictive. Delayed relaxation is characterized by prolonged isovolumic relaxation time

Address for reprint requests and other correspondence: S. J. Kovács, Cardiovascular Biophysics Laboratory, Box 8086, Barnes-Jewish Hospital at Washington University Medical Center, 660 South Euclid Ave., St. Louis, MO 63110 (E-mail: sjk@howdy.wustl.edu).

The costs of publication of this article were defrayed in part by the payment of page charges. The article must therefore be hereby marked "advertisement" in accordance with 18 U.S.C. Section 1734 solely to indicate this fact.

(IVRT), lower-than-normal E-wave and higher-than-normal A-wave amplitudes, and prolonged  $t_{dec}$ . The pseudonormalized pattern features increased E-wave amplitude due to elevated atrial pressure. Because this generates an increased atrioventricular pressure gradient, it “normalizes” the E-to-A ratio to  $>1$ . The restrictive pattern is characterized by short IVRT, a tall, narrow E wave with high peak velocity, short  $t_{dec}$  ( $<160$  ms), and a small A wave (2, 29), and it is usually associated with a third heart sound (S3) (18). The effects of compensatory mechanisms may mask the effects of diastolic dysfunction on the LV filling pattern and indicate a lack of specificity in the ability of a transmitral flow velocity-derived index, such as the E-to-A ratio, to quantitate specific physiological attributes such as chamber compliance or stiffness. For routine interpretation of transmitral Doppler waveforms, the differentiation between the effect of relaxation and compliance has been emphasized (2). In an effort to relate measures derived from the Doppler E wave to specific physiological chamber properties, Little et al. (17) proposed a method for measurement of LV chamber stiffness. In their study in dogs (17), average LV chamber stiffness  $[(\Delta P/\Delta V)_{avg}]$  was defined as the pressure change ( $\Delta P$ ) from minimum LVP to LVEDP divided by the change in LV volume during the same time interval. E-wave deceleration was modeled via the equation of motion (Newton’s law) for an undamped harmonic oscillator. When applied to the deceleration portion of the E wave, its solution related the rate of flow deceleration directly to atrial pressure and MV area and inversely to the sum of left atrial and LV stiffness, as previously modeled (20, 28). Solution of the differential equation predicted that the deceleration portion of the E wave should be well fit by a cosine function, the argument of which contained  $t_{dec}$ . The final result obtained by Little et al. predicted that chamber stiffness ( $K_{LV}$ ) could be calculated from  $t_{dec}$  of the Doppler E wave as follows

$$K_{LV} = [(\rho \cdot L)/(A)] \cdot [(\pi/2) \cdot (1/t_{dec})]^2 \quad (1)$$

where  $\rho$  is the density of blood,  $L$  is the effective, mitral “plug-flow” length, and  $A$  is the (constant) effective MV area. To validate the Doppler-predicted  $t_{dec}$ - $K_{LV}$  relation,  $(\Delta P/\Delta V)_{avg}$  was measured using micromanometric LVP values. The change in volume ( $\Delta V$ ) associated with  $\Delta P$  was based on an ellipsoidal model of the LV with axes corresponding to anterior-posterior, septal-lateral, and long-axis dimensions. A strong relationship was observed between the  $t_{dec}$ -predicted  $K_{LV}$  and  $(\Delta P/\Delta V)_{avg}$  invasively measured in eight dogs. Thus  $t_{dec}$  of the Doppler E wave was shown to be a noninvasive index of average chamber stiffness for E waves, for which (concave downward) the deceleration portion was well fit by a cosine function (17). Recently, using the same conceptual approach, Garcia et al. (5a) estimated LV operating stiffness from  $t_{dec}$  in 18 subjects undergoing open heart surgery.

For quantitative diastolic function assessment from Doppler echocardiography, a parameterized diastolic filling formalism has been developed and previously

validated (6, 7, 12). This model accounts for the mechanical suction attribute of the heart (11, 26) via a damped, simple harmonic oscillator as a paradigm for filling. The Doppler E-wave contour is the analog of the solution for velocity as a function of time to the equation of motion of the oscillator. According to Newton’s law, the equation of motion for the E wave is given by

$$m\ddot{x} + c\dot{x} + kx = 0 \quad (2)$$

where the overdot denotes differentiation with respect to time,  $m$  (in g) is inertia,  $c$  (in g/s) is the damping constant, and  $k$  (in g/s<sup>2</sup>) is the spring constant. For convenience, we set  $m = 1$  and compute parameters per unit mass. The oscillator springs back from non-zero ( $x_0$ , in cm) initial displacement (stored elastic strain) as transmitral flow commences. With the entire Doppler E-wave contour’s maximum velocity envelope (MVE) as input, a computer-based, automated, least-squares (Levenberg-Marquardt) fit of the model-predicted solution for velocity as a function of time solves the “inverse problem” of diastole and generates the three (unique) model parameters  $x_0$ ,  $k_E$ , and  $c$  (6, 7, 12). These three parameters account for the amplitude, width, and rate of decay of the E wave, respectively. For the A wave (7), the damped simple harmonic oscillator model utilizes a forcing function  $[F(t) = F_0 \sin(\omega t)]$ , the analog of atrial systole, and utilizes the parameters  $F_0$  and  $\omega$  (the magnitude and angular frequency of the forcing function,  $F$ ). This model-based image-processing (MBIP) strategy for analysis of Doppler E and A waves eliminates the need to digitize the contour by hand or determine its attributes such as maximum velocity, E-to-A ratio,  $t_{acc}$ , or  $t_{dec}$  by eye (Fig. 1).

The methods employed by Little et al. (17) indicated that the deceleration portion of the E wave (starting at the peak of the E wave) should be well fit by a cosine function, whereas the solution of Eq. 2 predicts that the entire E wave (starting at its onset) is well fit by the product of a sine function and a decaying exponential. It has been shown (14) that, for small values of the exponential decay term, the MBIP-predicted E-wave contour (sine wave, starting at the onset of the E wave) is equivalent to the cosine (starting at the peak of the E wave) fit to the deceleration portion of the E wave proposed by Little et al. The equivalence of sine to cosine (shifted by  $\pi/2$  rad) permits derivation of an exact algebraic relationship relating  $t_{dec}$  (and  $K_{LV}$ ) as employed by Little et al. to  $k_E$  of the parameterized diastolic filling model. For validation, transmitral Doppler images were subjected to MBIP, and the predicted linear relationship between  $K_{LV}$  and  $k_E$  has been previously verified (14).

To validate the predicted linearity of the (E-wave-generated)  $k_E$ - $(\Delta P/\Delta V)_{avg}$  relation, simultaneous LVP and transmitral flow data were obtained in 131 subjects exhibiting a broad range of E-wave patterns. The method also permitted determination of chamber stiffness during early rapid filling  $(\Delta P/\Delta V)_E$  and its correlation to  $k_E$ . In those having a period of diastasis, passive chamber stiffness,  $k_A$ , was determined from

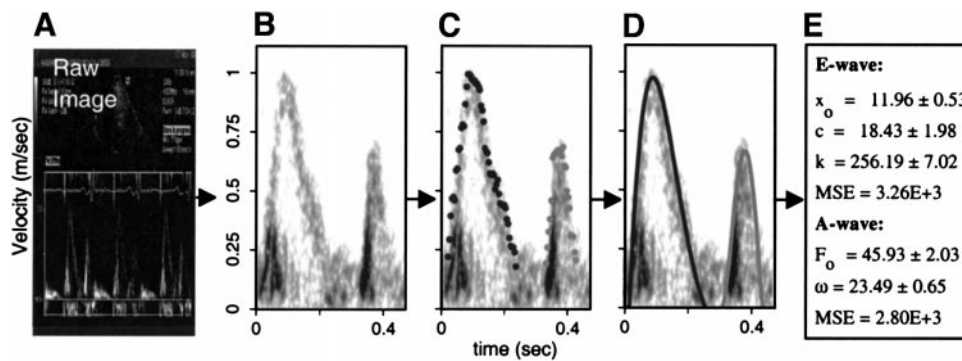


Fig. 1. Overview of the model-based image-processing (MBIP) method of model fitting and parameter determination with the Doppler image as input. Sequence of steps is as follows: acquire digital transmitral Doppler image (A), select diastolic interval of interest (B), determine maximum velocity envelope to be used as input for MBIP (C), and perform fit using Levenberg-Marquardt method (D). E: results, i.e., parameter values and standard deviations, including mean square error (MSE) as a measure of goodness of fit.  $x_0$ , initial displacement (cm);  $c$ , damping constant (g/s);  $k$ , spring constant (g/s<sup>2</sup>),  $F_0$ , magnitude (dyn);  $\omega$ , angular frequency (rad/s).

the A wave and compared with postdiastasis stiffness  $[(\Delta P/\Delta V)_{PD}]$ .

### Glossary

LV	Left ventricular
$K_{LV}$	Chamber stiffness computed by Little et al. (17) (mmHg/cm <sup>3</sup> )
$t_{dec}$	Deceleration time (s)
$(\Delta P/\Delta V)_{avg}$	Average chamber stiffness (mmHg/cm <sup>3</sup> )
$(\Delta P/\Delta V)_E$	Chamber stiffness of early rapid filling (mmHg/cm <sup>3</sup> )
$(\Delta P/\Delta V)_{PD}$	Passive (postdiastasis) chamber stiffness (mmHg/cm <sup>3</sup> )
MV	Mitral valve
$m$	Mass (g)
$c$	Damping constant (g/s)
$k$	Spring constant (linear form; g/s <sup>2</sup> )
$x$	Displacement (cm)
$x_0$	Initial displacement (displacement at $t = 0$ ; cm)
MBIP	Model-based image processing
$k_E$	Stiffness parameter for the Doppler E wave (g/s <sup>2</sup> )
$k_A$	Stiffness parameter for the Doppler A wave (g/s <sup>2</sup> )
TVI	Time-velocity integral
MSE	Mean square error
MVE	Maximum velocity envelope
LVP	LV pressure (mmHg)
LVEDP	LV end-diastolic pressure (mmHg)
IVRT	Isovolumic relaxation time (s)

### METHODS

**Clinical data acquisition.** Simultaneous transmitral Doppler and high-fidelity hemodynamic (LVP) data were obtained in 131 patients undergoing elective cardiac catheterization at the request of their referring physician. Informed consent was obtained in accordance with Washington University Medical Center Human Studies Committee guidelines. All subjects were in sinus rhythm. None of the subjects had any significant valvular abnormality. Simultaneous hemodynamic and Doppler echocardiographic data were acquired

before injection of iodinated contrast for selective coronary angiography and left ventriculography. Subjects were sedated with diazepam (2.5–5.0 mg iv). Left ventriculography was performed in the conventional 30° right anterior oblique view using a power injector (Mark V, MedRad) via a 7-Fr pigtail catheter (Millar, Houston, TX).

Short-axis parasternal views for effective MV area determination and transmitral pulsed-Doppler flow velocity images were obtained according to standard criteria (3). The sample volume was located at the mitral leaflet tips in the four-chamber apical view. Imaging was performed using an echocardiographic imaging system (model C256, Acuson Sequoia, Mountain View, CA) equipped with a 2-MHz transducer. Between 20 and 30 consecutive beats were digitally stored in the imager's memory and downloaded to magneto-optical disks. Simultaneous micromanometric LVP values were obtained using a 7-Fr pigtail catheter (model 747P, Millar). LVP and electrocardiogram data were subjected to analog-to-digital conversion at a sampling rate of 1 kHz with a digitizing board (model MIO-16XE, National Instruments, Austin, TX) and were acquired in LabView resident on a 200-MHz Power Macintosh 7200 computer with 128 megabytes of random access memory and 500 megabytes of hard drive. Pressure and transmitral Doppler image data were synchronized by a square-wave fiducial marker. Additionally, simultaneous electrocardiogram traces were recorded as part of pressure and flow data sets. Analysis was performed off-line in the Cardiovascular Biophysics Laboratory.

**MBIP.** Transmitral Doppler E and A waves were subjected to MBIP as previously described (6, 7, 12, 14) for model parameter determination (Fig. 1). We also previously showed that averaging of parameters from individual images is superior to averaging of images, with an average variation of <10% for all parameters (8, 9). Accordingly, individual beats were selected from the original transmitral digital Doppler image data set. To account for beat-to-beat variability, at least five beats per subject underwent MBIP, and the resulting parameters were averaged (8, 9).

Examples of model fit to a range of transmitral Doppler images with corresponding MBIP-derived parameters are displayed in Fig. 2. For E waves, model fit is not restricted to concave-downward deceleration segments only (cosine shapes) but includes E-wave patterns having an inflection point in the deceleration portion. Independently,  $t_{dec}$  was determined for each of the E waves by two methods. The first

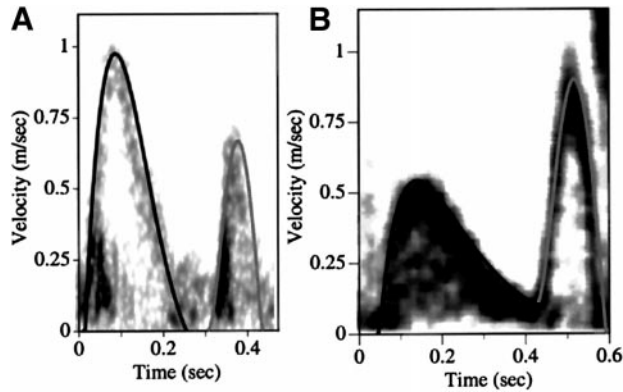


Fig. 2. Selected examples of in vivo Doppler transmitral flow velocity images obtained during cardiac catheterization. A: E wave having a deceleration portion well fit by a cosine function and the MBIP-predicted contour. This deceleration contour is similar to E-wave shapes considered in the canine study by Little et al. (17). B: E wave having an inflection point during the deceleration portion. Fit generated by the MBIP method is superimposed.

used the conventional method (7) of extending the deceleration portion from the peak of the E wave as a straight line to the velocity = 0 axis. The second, automated method used the MBIP-predicted contour and computed the elapsed time from its peak to its intersection with the velocity = 0 axis. The  $t_{dec}$  was used to compute  $K_{LV}$  using Eq. 1.

**Average chamber stiffness.** Average chamber stiffness was defined as the ratio of the change in pressure to the change in volume  $[(\Delta P/\Delta V)_{avg}]$  during the time interval from minimum LVP to LVEDP, as defined by Little et al. (17). Briefly,  $(\Delta P)_{avg}$  was defined as the difference between minimum LVP and LVEDP for the same beats subjected to MBIP. An example of the micromanometric LVP trace from a single individual and the simultaneous transmitral Doppler image are shown in Fig. 3. The pressure portion utilized for determination of  $(\Delta P)_{avg}$  is shown in Fig. 3C.  $(\Delta V)_{avg}$  was calculated by using the sum of the time-velocity integral (TVI) for the E and A waves commencing from the time of minimum LVP to LVEDP. To obtain the corresponding change in volume, the two-dimensional echocardiographic effective MV area was multiplied by the TVI.  $\Delta V$  as a function of time is shown in Fig. 3B. The effective MV area is the echocardiographic annular area multiplied by the (dimensionless) factor R ( $R < 1$ ), where R is the ratio of annular area E- and A-wave TVI to leaflet tip E- and A-wave TVI. The Doppler E-wave (MBIP)-derived parameter  $k_E$  was plotted vs. the invasively obtained  $(\Delta P/\Delta V)_{avg}$  for each subject. To facilitate direct comparison with the method of Little et al. (17),  $t_{dec}$  was measured directly, allowing determination of  $K_{LV}$ . This allowed experimental validation of the theoretically predicted (14) linear relationship of  $k_E$  to  $K_{LV}$ .

**Early rapid-filling stiffness.** Stiffness during the E-wave interval (E-wave stiffness) was defined as the change in pressure divided by the change in volume  $[(\Delta P/\Delta V)_E]$  for the interval from minimum LVP to LVP at diastasis. The E-wave-derived stiffness parameter  $k_E$  was plotted vs.  $(\Delta P/\Delta V)_E$  [see Fig. 3 for graphical definition of  $(\Delta P)_E$  and  $(\Delta V)_E$ ].

**Passive chamber stiffness.** Passive chamber stiffness was determined for subjects having a period of diastasis. Presence of diastasis indicated a period of no (or insignificant) transmitral flow, i.e., abolition of the atrioventricular pressure gradient with concomitant equilibration of residual atrioventricular forces. Passive chamber stiffness after diastasis was defined by the ratio of change in pressure to change

in volume due to atrial systole  $[(\Delta P/\Delta V)_{PD}]$ ; Fig. 3]. In analogy to the relationship of  $k_E$  to E-wave-determined stiffness, we sought to validate the prediction that the A-wave-derived parameter  $k_A$  is linearly related to the passive chamber

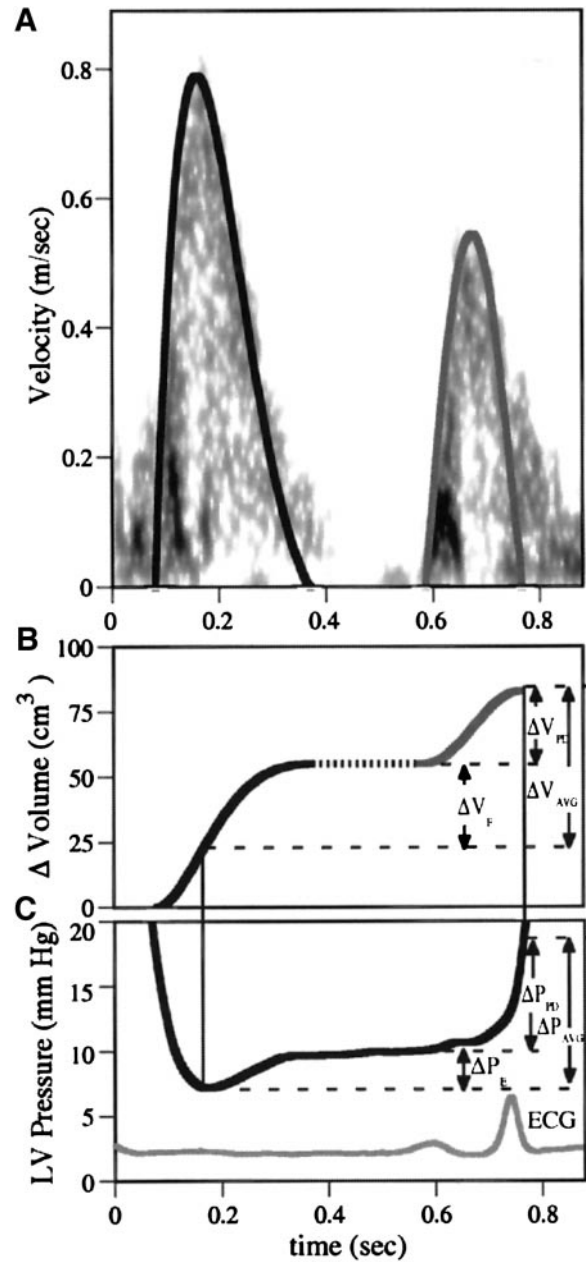


Fig. 3. Selected Doppler image and a portion of the simultaneous micromanometric left ventricular pressure (LVP) trace used for computation of chamber stiffness  $(\Delta P/\Delta V)$ , where P is pressure and V is volume) for selected phases of filling. A: simultaneous transmitral flow velocity as imaged by Doppler echocardiography. B: change in LV volume as a function of time since mitral valve opening. According to Little et al. (17),  $(\Delta V)_{avg}$  is defined as the volume change during the minimum LVP to LV end-diastolic pressure (LVEDP) interval.  $(\Delta V)_E$  and  $(\Delta V)_{PD}$ , volume changes during the E-wave and atrial contraction portions, respectively. C: high-fidelity recording of LVP. Single diastolic interval is shown.  $(\Delta P)_{avg}$ , rise in pressure from minimum LVP to LVEDP;  $(\Delta P)_E$ , rise in pressure from minimum LVP to the end of the E wave (diastasis in this case);  $(\Delta P)_{PD}$ , postdiastatic rise in pressure due to atrial systole; ECG, electrocardiogram.

stiffness. Accordingly, the relationship of  $k_A$  to  $(\Delta P/\Delta V)_{PD}$  was compared. Linear least-squares best fit and corresponding  $r$  value were determined using DeltaGraph for echo-derived vs. invasively derived definitions of stiffness for the above-defined average, early rapid-filling, and passive (post-diastasis) phases of filling.

## RESULTS

**Group attributes.** LV ejection fraction (LVEF) as determined by ventriculography for the entire group was normal:  $70 \pm 12\%$  (SD). Additional characteristics of the sample include gender (85 men and 46 women), age ( $53 \pm 10$  yr), heart rate ( $68 \pm 12$  beats/min), and LVEDP ( $17 \pm 5$  mmHg). MBIP-derived fits of the predicted velocity contours to the clinical Doppler E-wave images showed excellent agreement. For all ( $n = 131$ ) subjects, the average mean squared error (MSE) was  $7.23 \times 10^{-4}$  for the E wave and  $6.14 \times 10^{-4}$  for the A wave. The ability to compute a measure of goodness of fit in the form of MSE is an inherent advantage of the MBIP approach. Figure 2 illustrates model-predicted transmitral flow velocity superimposed onto selected clinical E and A waves. Least-squares linear best fit and correlation coefficient in this human study were determined in analogy to the study by Little et al. (17) in their canine model. In addition, the method and the data set permitted noninvasive prediction and invasive validation of stiffness during selected phases of diastole. Specifically, the Doppler-derived early rapid-filling stiffness,  $k_E$ , could be compared with  $(\Delta P/\Delta V)_E$ , and (postdiastasis) chamber stiffness,  $k_A$ , could be compared with  $(\Delta P/\Delta V)_{PD}$ . In analogy to Little and Downes (16), Fig. 4 displays the data for the echocardiographically determined parameter  $k_E$  and its relation to the simultaneous, invasively determined average stiffness:

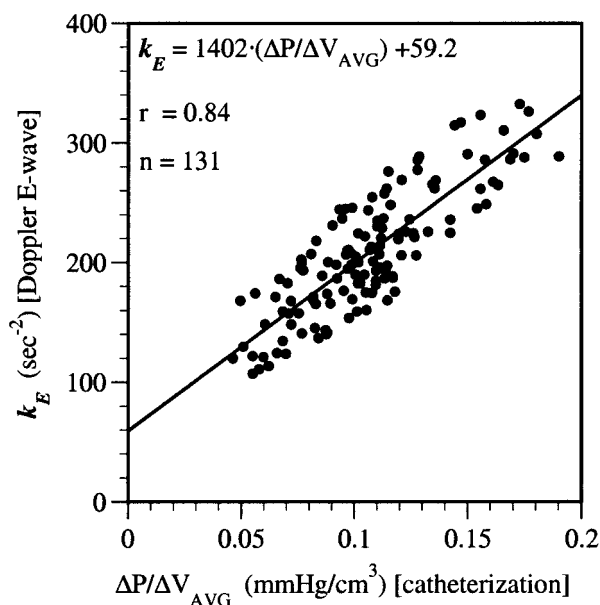


Fig. 4. MBIP-generated, Doppler E-wave-derived parameter ( $k_E$ ) vs. invasively determined average chamber stiffness  $[(\Delta P/\Delta V)_{avg}]$  for 131 subjects. Best fit was provided by  $k_E = 1,402 \cdot (\Delta P/\Delta V)_{avg} + 59.2$  ( $r = 0.84$ ).

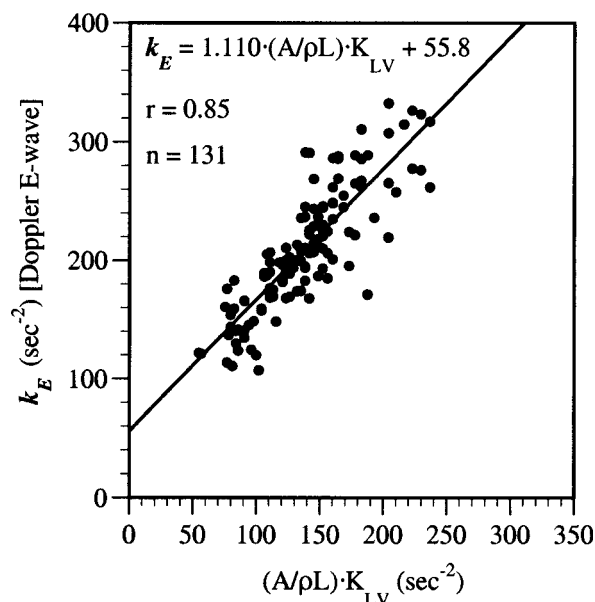


Fig. 5. MBIP-generated  $k_E$  vs. invasively determined chamber stiffness ( $K_{LV}$ ) based on deceleration time ( $t_{dec}$ ) of the Doppler E-wave for 131 subjects. Best fit was provided by  $k_E = 1.110 \cdot (A/\rho L) \cdot K_{LV} + 55.8$ , where  $A$  is (constant) effective mitral valve area,  $L$  is effective mitral “plug-flow” length, and  $\rho$  is density of blood ( $r = 0.85$ ).

$K_{LV} = (\Delta P/\Delta V)_{avg}$ . Linear regression, with least MSE best fit ( $n = 131$ ), yielded  $k_E = 1,402 \cdot (\Delta P/\Delta V)_{avg} + 59.2$  with strong correlation ( $r = 0.84$ ). The E-wave stiffness parameter  $k_E$  is compared with  $K_{LV}$  of Little and Downes as determined by  $t_{dec}$  of the Doppler E wave in Fig. 5. Linear regression yielded  $k_E = 1.110 \cdot (A/\rho L) \cdot K_{LV} + 55.8$  ( $r = 0.85$ ). Figure 6 depicts  $k_E$  vs.  $(\Delta P/\Delta V)_E$ . Linear regression yielded  $k_E = 229.0 \cdot (\Delta P/\Delta V)_E + 112$  ( $r = 0.80$ ). Figure 7 depicts the Doppler A-wave-derived parameter  $k_A$  vs.  $(\Delta P/\Delta V)_{PD}$ . Linear regression yields  $k_A = 1,640 \cdot$

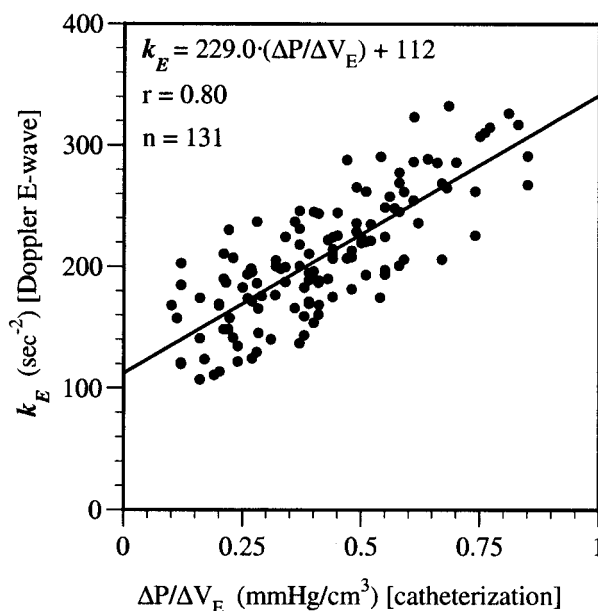


Fig. 6. MBIP-generated  $k_E$  vs. invasively determined early rapid filling chamber stiffness  $[(\Delta P/\Delta V)_E]$  for 131 subjects. Best fit was provided by  $k_E = 229.0 \cdot (\Delta P/\Delta V)_E + 113$  ( $r = 0.80$ ).

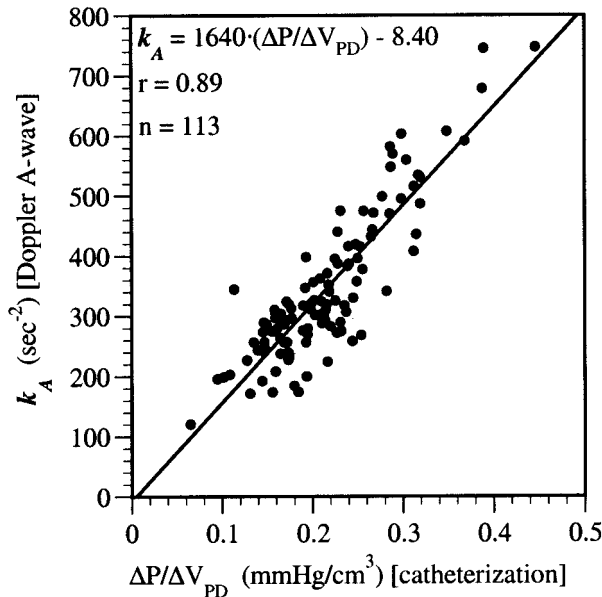


Fig. 7. MBIP-generated, Doppler A-wave-derived parameter ( $k_A$ ) vs. invasively determined passive chamber stiffness  $[(\Delta P/\Delta V)_{PD}]$  for 113 subjects with diastasis. Best fit was provided by  $k_A = 1,640 \cdot (\Delta P/\Delta V)_{PD} - 8.40$  ( $r = 0.89$ ).

$(\Delta P/\Delta V)_{PD} - 8.40$  ( $r = 0.89$ ). Figure 8 combines Figs. 4, 6, and 7 and indicates the following order: slope of the linear regression relation for early stiffness < slope for average stiffness < slope for postdiastasis stiffness. This is consistent with the concave-upward shape of the LV diastolic pressure-volume curve.

**DISCUSSION**

The quest for Doppler-derived physiological indexes of diastolic function has remained an area of active investigation (22). Progress has been made through mathematical modeling of diastolic physiology, which provided quantitative insight into how Doppler E-wave contours are determined by the transmitral atrioventricular pressure gradient (15). In turn, how the atrioventricular pressure gradient depended on numerous physiological variables, such as atrial stiffness and capacitance as well as MV inertance and chamber properties, has been also described in detail (19, 21, 24, 27, 30). One inherent limitation of the (nonlinear) physiological modeling approaches is their inability to use the clinical Doppler contour as input to generate unique model parameters as output (23). Our approach circumvents this limitation by approximating the filling process by the use of a linear model for filling. This requires the lumping of all physiological determinants of transmitral flow for the E wave into three parameters to account for its amplitude ( $x_o$ ), width ( $k_E$ ), and rate of decay ( $c$ ). The goodness of the model-predicted fit to in vivo contours underscores the utility of the approach as a practical tool for analysis and for facilitation of clinical decisions by accommodating the full range of Doppler flow velocity patterns encountered in vivo (13, 25).

As a result of the pioneering work of Little et al. (17) in a canine model, additional progress toward physiological interpretation of E-wave attributes has been achieved by their theoretical derivation and validation of a relationship between E-wave  $t_{dec}$  and chamber stiffness. On the basis of their work, we previously established a direct linear relationship between the E-wave-determined parameter  $k_E$  and their  $t_{dec}$ -derived chamber stiffness  $K_{LV}$  (14). A minor difference between the study of Little et al. and this study is that the entire E wave is used as input to the model, instead of only the  $t_{dec}$  (2 points of the entire contour). This has the advantage of using more information to fit the model-predicted contour, thereby providing a more powerful analysis. On the other hand, it has the shortcoming of requiring computation that cannot be simply performed by inspection of the Doppler contour. Testing the analogous ( $k_E$ -average stiffness relation) hypothesis in humans, extending it to include E-wave patterns having an inflection point in the deceleration portion, and being able to consider the early rapid-filling and the late, postdiastatic (passive) stiffness phases of diastole represent the focus of the present in vivo work. One key result (Fig. 4) relates invasive and noninvasive determination of (average) chamber stiffness in vivo in humans ( $n = 131$ ). Figure 4 is the analog of the experimentally determined relationship observed in a canine model ( $n = 8$ ) by Little et al. (17). In agreement with the canine study, a linear correlation was found.

The MBIP strategy eliminates the need to quantify the transmitral Doppler contour or determine its attributes (e.g.,  $t_{acc}$ ,  $t_{dec}$ , E-to-A ratio) "by eye." Figure 2

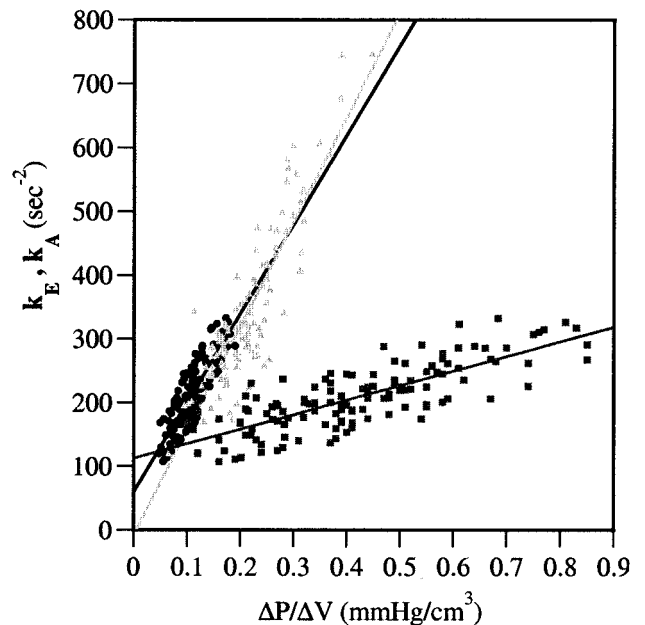


Fig. 8. MBIP-generated, Doppler-derived parameters vs. invasively determined chamber stiffness for  $k_E$  vs.  $(\Delta P/\Delta V)_{avg}$  ( $\bullet$ ),  $k_E$  vs.  $(\Delta P/\Delta V)_E$  ( $\blacksquare$ ), and  $k_A$  vs.  $(\Delta P/\Delta V)_{PD}$  ( $\blacktriangle$ ). Overall, average stiffness of the ventricle is considerably greater during atrial contraction than during early filling, and average stiffness (which lumps the 2 phases together) falls between early and late stiffness values.

illustrates typical E-wave images demonstrating excellent agreement between model prediction and the clinical velocity contour. Furthermore, the predicted linear correlation between the noninvasively determined parameter  $k_E$  and the invasively determined  $(\Delta P/\Delta V)_{\text{avg}}$ , between  $k_E$  and  $K_{LV}$ , between  $k_E$  and early rapid-filling stiffness, and between  $k_A$  and postdiastolic stiffness has been validated in a large in vivo sample having a broad distribution of Doppler flow velocity patterns.

Although a strong correlation is observed indicating that  $k_E$  is a clinically viable noninvasive estimate of average chamber stiffness and that  $k_A$  is an excellent estimate of passive chamber stiffness, some limitations remain.

*Limitations.* The limitations encountered in this study fall into two categories: methodological and conceptual.

One minor methodological limitation is the lack of individual pressure or volume alteration in the subjects studied. Ideally, to determine the diastolic pressure-volume relation and its slope  $\Delta P/\Delta V$  at any point along the pressure-volume curve for an individual subject, manipulation of pressure by pharmacological means (pressors or nitroglycerine) or alteration of volume (by volume loading or inferior vena cava occlusion) could be performed. These manipulations permit determination of the entire diastolic pressure-volume relation for an individual subject. Although these manipulations were not part of our protocol for  $\Delta P/\Delta V$  determination in the subjects undergoing elective diagnostic cardiac catheterization, measurement of  $(\Delta P/\Delta V)_{\text{avg}}$  as performed by Little et al. and determination of  $(\Delta P/\Delta V)_E$  and  $(\Delta P/\Delta V)_{PD}$  permitted their respective determinations for each subject at the operational point along each individual's pressure-volume curve. This is justified, since our goal was not determination of the entire pressure-volume relation for each subject but determination of the echocardiographically determined average, early rapid-filling, or passive chamber stiffness for a single diastole and its relation to the invasively determined  $\Delta P/\Delta V$  for the same diastole. The large number of subjects studied ( $n = 131$ ) and inclusion of E-wave patterns having an inflection point in their deceleration portions extended the range of  $t_{\text{dec}}$  and stiffnesses encountered.

Another minor methodological limitation concerns the reproducibility of locating the micromanometric pressure transducer at the mid-LV level. Because diastolic intraventricular pressure gradients exist (5), LVP contours depend somewhat on the base-to-apex location of the transducer. Our primary criterion for mid-LV transducer location was modulated by our desire to prevent catheter-induced ectopy. Variation in pressure transducer location introduces some variability into our measurement of  $\Delta P$ , particularly during the E wave and likely contributes to the slightly lower ( $r = 0.84$ ) correlation observed in this study compared with the correlation ( $r = 0.92$ ) observed in the canine study by Little et al. (17). During passive filling due to atrial systole, intraventricular gradients are diminished; hence, reproducible catheter location has less effect on

determination of  $\Delta P$ , likely contributing to the higher correlation we observed ( $r = 0.89$ ).

Our study may be subject to the concern that we did not select, sort, or analyze our data according to clinical subset criteria such as hypertension, diabetes, or ischemic heart disease or group them according to the presence of various pharmacological therapies (e.g., angiotensin-converting enzyme inhibitors,  $\beta$ -blockers, diuretics). Treating all subjects as a single group is justified by our goal to validate the predicted physiological relationship between invasively determined average, early rapid-filling, or passive stiffness and the simultaneously determined noninvasive chamber stiffness,  $k_E$  or  $k_A$ , in a broad in vivo sample. This relationship is derived from the biophysical rules of filling, which all hearts obey, rather than the type of pathology or medication that may or may not be present. We wish to emphasize that our findings in this group of patients have yet to be further validated in specific pathophysiological subsets having abnormally low LVEF or abnormally high LVEDP. Determination of the relationship of average, early rapid-filling, or passive chamber stiffness as a function of pathological state and pharmacological intervention is an interesting and justified subject for future studies.

A conceptual limitation relates to the definition of average stiffness as  $(\Delta P/\Delta V)_{\text{avg}}$  and the recognition that  $\Delta P$  (defined as the difference between LVEDP and minimum LVP) utilized in this study and in the prior study by Little et al. (17) does not correspond to the entire duration of filling, because it omits the period of filling from MV opening to minimum LVP. When ventricular filling (Doppler E wave) begins, LVP continues to diminish ( $dP/dt < 0$ ) as LV volume rapidly increases ( $dV/dt > 0$ ) (18, 29). By definition,  $dP/dV$  (stiffness) during this interval (of mechanical suction) is negative. Negative stiffness in and of itself is not a cause for conceptual difficulty because it indicates that the recoiling chamber is doing external work (mechanical suction) on atrioventricular blood. After minimum LVP is reached, stiffness changes sign and becomes positive, indicating that the fluid, having reached maximum velocity, is doing external (inertia generated) work on the chamber by distending it and raising its pressure. Because  $(\Delta P/\Delta V)_{\text{avg}}$  was defined as starting at minimum LVP (16), the suction-initiated (negative stiffness) portion of early filling is neglected. In addition,  $\Delta V$  was calculated commencing at the corresponding portion (minimum LVP) of the E wave and including all the A wave. The advantage of opting for the above choice for average stiffness is that it confines analysis to the  $\Delta P/\Delta V > 0$  portion of the diastolic interval (Fig. 3). The physiological and conceptual limitation is that it combines (suction initiated, inertia and relaxation modulated) stiffness during the latter half of the E wave with (passive) postdiastolic stiffness during the A wave. We were able to address this conceptual limitation in this study by considering the  $k_E-(\Delta P/\Delta V)_E$  and the  $k_A-(\Delta P/\Delta V)_{PD}$  relations separately. Our measurements showing a high correlation of  $k_E$  to  $(\Delta P/\Delta V)_{\text{avg}}$  but an even higher correlation of  $k_A$  to  $(\Delta P/\Delta V)_{PD}$

suggest that lumping early and late diastolic stiffness into a single averaged stiffness parameter introduces a slight variation. The separation of early and passive chamber stiffness manifests as a nonzero intercept of the linear regression relation in Fig. 6 compared with the (essentially) zero intercept in Fig. 7. The nonzero  $y$ -intercept for early rapid filling reflects the effect of determining stiffness while filling is already in progress. Note that stiffness changes sign from  $\Delta P/\Delta V < 0$  (from MV opening to minimum LVP) to  $\Delta P/\Delta V > 0$  (from minimum LVP to the end of the E wave). In comparison, for passive stiffness, flow velocity starts from zero and ends at zero (duration of the A wave), and the sign of  $\Delta P/\Delta V$  remains  $> 0$  throughout. As expected on conceptual grounds, maintaining the distinction between E wave (suction-initiated) and postdiastasis A wave (passive) stiffness yields a better correlation between noninvasive prediction and invasive validation.

**Conclusion.** This study validates the model-predicted linear relationship between the MBIP-determined, E-wave-based  $k_E$  and the simultaneous, invasively obtained  $(\Delta P/\Delta V)_{\text{avg}}$ . Our results in humans are in concert with the work of Little et al. (17) in a canine model. We found the relationship to be  $k_E = 1,402 \cdot (\Delta P/\Delta V)_{\text{avg}} + 59.2$  with good correlation ( $r = 0.84$ ). Such validation has not been previously performed in a large sample ( $n = 131$ ) of human subjects having normal LVEF. The model-predicted linear relationship of  $k_E$  to  $(\Delta P/\Delta V)_E$  was also validated and observed to be  $k_E = 229.0 \cdot (\Delta P/\Delta V)_E + 112$  with good correlation ( $r = 0.80$ ). In addition, the prediction that postdiastasis A-wave-based  $k_A$  is linearly related to  $(\Delta P/\Delta V)_{\text{PD}}$  was validated:  $k_A = 1,640 \cdot (\Delta P/\Delta V)_{\text{PD}} - 8.40$  with excellent correlation ( $r = 0.89$ ). These results establish new tools by which average, early rapid-filling, and passive (postdiastasis) chamber stiffness may be noninvasively attained on a beat-by-beat basis in vivo. The findings underscore the role that all hearts play as mechanical suction pumps in early diastole and strengthen our understanding of the relationship between Doppler echo-derived parameters and their in vivo physiological analogs.

Helpful discussions with Stephanie Eucker, Mark Sessoms, and Michael Courtois are appreciated. Echocardiographic data acquisition would not have been possible without the skilled contributions of Peggy Brown. The assistance of the nursing and technical staff of the Barnes-Jewish Hospital Cardiac Catheterization Laboratory is gratefully acknowledged.

This work was supported in part by the Whitaker Foundation (Roslyn, VA), National Heart, Lung, and Blood Institute Grants HL-54179 and HL-04023, and the Alan A. and Edith L. Wolff Charitable Trust (St. Louis, MO).

## REFERENCES

1. **Appleton CP.** The hemodynamic determinants of Doppler pulmonary venous flow velocity components: new insights from studies in lightly sedated dogs. *J Am Coll Cardiol* 30: 1562–1574, 1997.
2. **Appleton CP, Firstenberg MS, Garcia MJ, and Thomas JD.** The echo-Doppler evaluation of left ventricular diastolic function: a current perspective. In: *Diastolic Function and Dysfunction*, edited by Kovács SJ. Philadelphia, PA: Saunders, 2000, p. 513–546.
3. **Appleton CP, Jensen JL, Hatle LK, and Oh JK.** Doppler evaluation of left and right ventricular diastolic function: a technical guide for obtaining optimal flow velocity recordings. *J Am Soc Echocardiogr* 10: 271–291, 1997.
4. **Caulfield JB and Janicki JS.** Structure and function of myocardial fibrillar collagen. *Technol Health Care* 5: 95–113, 1997.
5. **Courtois MR, Kovács SJ Jr, and Ludbrook PA.** The diastolic atrioventricular relationship is a function of the site of pressure measurement in the left ventricle (Abstract). *Circulation* 76: IV-426, 1987.
- 5a. **Garcia MJ, Firstenberg MS, Greenberg NL, Smedira N, Rodriguez L, Prior D, and Thomas JD.** Estimation of left ventricular operating stiffness from Doppler early filling deceleration time in humans. *Am J Physiol Heart Circ Physiol* 280: H554–H561, 2001.
6. **Hall AF, Aronovitz JA, Nudelman SP, and Kovács SJ.** Automated method for characterization of diastolic transmitral Doppler velocity contours: late atrial filling. *Ultrasound Med Biol* 20: 859–869, 1994.
7. **Hall AF and Kovács SJ.** Automated method for characterization of diastolic transmitral Doppler velocity contours: early rapid filling. *Ultrasound Med Biol* 20: 107–116, 1994.
8. **Hall AF, Nudelman SP, and Kovács SJ.** Beat averaging alternatives for transmitral Doppler flow velocity images. *Ultrasound Med Biol* 7: 971–979, 1998.
9. **Hall AF, Nudelman SP, and Kovács SJ.** Evaluation of model-based processing algorithms for averaged transmitral spectral Doppler images. *Ultrasound Med Biol* 24: 55–66, 1998.
10. **Helmes M, Trombitás K, and Granzier H.** Titin develops restoring force in rat cardiac myocytes. *Circ Res* 79: 619–626, 1996.
11. **Katz LN.** The role played by the ventricular relaxation process in filling the ventricle. *Am J Physiol* 95: 542–553, 1930.
12. **Kovács SJ, Barzilai B, and Pérez JE.** Evaluation of diastolic function with Doppler echocardiography: the PDF formalism. *Am J Physiol Heart Circ Physiol* 252: H178–H187, 1987.
13. **Kovács SJ, Rosado J, Manson-McGuire AL, and Hall AF.** Can transmitral Doppler E-waves differentiate hypertensive hearts from normal? *Hypertension* 30: 788–795, 1997.
14. **Kovács SJ, Setser R, and Hall AF.** Left ventricular chamber stiffness from model-based image processing of transmitral Doppler E-waves. *Coron Artery Dis* 8: 179–187, 1997.
15. **Kovács SJ, Yellin E, and Meisner J.** Modeling of diastole. In: *Diastolic Function and Dysfunction*, edited by Kovács SJ. Philadelphia, PA: Saunders, 2000, p. 459–490.
16. **Little WC and Downes TR.** Clinical evaluation of left ventricular diastolic performance. *Prog Cardiovasc Dis* 32: 273–290, 1990.
17. **Little WC, Ohno M, Kitzman DW, Thomas JD, and Cheng CP.** Determination of left ventricular chamber stiffness from the time of deceleration of early left ventricular filling. *Circulation* 92: 1933–1939, 1995.
18. **Manson AL, Nudelman SP, Hagley MT, Hall AF, and Kovács SJ.** Relationship of the third heart sound to transmitral flow velocity deceleration. *Circulation* 92: 388–394, 1995.
19. **Mirsky I.** Assessment of diastolic function: suggested methods and future considerations. *Circulation* 69: 836–841, 1984.
20. **Myreng Y and Smiseth OA.** Assessment of left ventricular relaxation by Doppler echocardiography: comparison of isovolumic relaxation time and transmitral flow velocities with time constant of isovolumic relaxation. *Circulation* 81: 260–266, 1990.
21. **Nikolic S, Yellin EL, Tamura K, Vetter H, Tamura T, Meisner JS, and Frater RW.** Passive properties of canine left ventricle: diastolic stiffness and restoring forces. *Circ Res* 62: 1210–1222, 1988.
22. **Nishimura RA and Tajik AJ.** Evaluation of diastolic filling of the left ventricle in health and disease: Doppler echocardiography is the clinician's Rosetta stone. *J Am Coll Cardiol* 30: 8–18, 1997.

23. **Nudelman S, Manson AL, Hall AF, and Kovács SJ Jr.** Comparison of diastolic filling models and their fit to transmitral Doppler contours. *Ultrasound Med Biol* 8: 989–999, 1995.
24. **Omens JH and Fung YC.** Residual strain in the rat left ventricle. *Circ Res* 66: 37–45, 1990.
25. **Rich MW, Stitzel NO, and Kovács SJ.** Prognostic value of diastolic filling parameters derived using a novel image processing technique in patients  $\geq 70$  years of age with congestive heart failure. *Am J Cardiol* 84: 82–86, 1999.
26. **Robinson TF, Factor SM, and Sonnenblick EH.** The heart as a suction pump. *Sci Am* 254: 84–91, 1986.
27. **Sun Y, Sjoberg BJ, Ask P, Loyd D, and Wranne B.** Mathematical model that characterizes transmitral and pulmonary venous flow velocity patterns. *Am J Physiol Heart Circ Physiol* 268: H476–H489, 1995.
28. **Thomas JD, Newell JB, Choong CY, and Weyman AE.** Physical and physiological determinants of transmitral velocity: numerical analysis. *Am J Physiol Heart Circ Physiol* 260: H1718–H1731, 1991.
29. **Thomas JD and Weyman AE.** Echocardiographic Doppler evaluation of left ventricular diastolic function: physics and physiology. *Circulation* 84: 977–990, 1991.
30. **Yellin EL, Hori M, Yoran C, Sonnenblick EH, Gabbay S, and Frater RW.** Left ventricular relaxation in the filling and nonfilling intact canine heart. *Am J Physiol Heart Circ Physiol* 250: H620–H629, 1986.

